Journal of Alloys and Compounds 509 (2011) 2970–2975

Contents lists available at ScienceDirect

Journal of Alloys and Compounds

journal homepage: www.elsevier.com/locate/jallcom

Confined growth of CuO, NiO, and Co_3O_4 nanocrystals in mesoporous silica (MS) spheres

Jie Zong, Yihua Zhu*, Xiaoling Yang, Chunzhong Li*

Key Laboratory for Ultrafine Materials of Ministry of Education, School of Materials Science and Engineering, East China University of Science and Technology, 130 Meilong Road, Shanghai 200237, China

ARTICLE INFO

Article history:
Received 22 July 2010
Received in revised form
23 November 2010
Accepted 25 November 2010
Available online 3 December 2010

Keywords:
Nanocrystals
Mesoporous silica (MS) spheres
Confined growth
Composite microspheres
Cyclic voltammograms

ABSTRACT

The confined growth of CuO, NiO, and Co_3O_4 nanocrystals in the mesopores of the MS spheres with the help of polyelectrolyte (PE) multilayers by calcination method has been investigated. Measurements and analyses of SEM, XRD, TEM, and TGA showed that the metal oxide (CuO, NiO, or Co_3O_4) nanoparticles were almost confined in the mesopores of the MS spheres and had good crystallinity. And the resulting composite microspheres with good dispersion are still mesoporous. This approach can be used to prepare composite materials involving metal oxide nanaoparticles, which have potential application in catalytic field. And the results showed that cyclic voltammograms (CV) were valuable for the investigation of catalytic performances of CuO/MS, NiO/MS, and Co_3O_4/MS composite microspheres.

1. Introduction

Metal oxide nanoparticles are widely used in many technological applications, such as coating [1,2], catalysis [3–5], electrode materials [6], sensors [7–9], and so on [10,11]. But physical and chemical properties of metal oxide nanoparticles are strongly influenced by their aggregation. And it has been demonstrated that the loading of pure metal oxide nanoparticles or their mixed oxides on to the inert support materials with high surface areas to form composite materials could help to prevent their aggregation and improve their chemical reactivity and stability [12].

Mesoporous silica materials, such as MCM-41, SBA-15 and KIT-6 are considered as ideal hosts for loading metal oxide particles due to its high surface area, large pore volume and uniform pore size distribution [13–19]. Moreover, mesoporous silica materials show some advantages such as low cost, wide availability and stability [20]. Therefore, much attention has been attracted to composites with metal oxide nanoparticles or their mixed oxides loading on the typical mesoporous silica materials recently. For example, Hernández-Pineda et al. prepared PdO/MCM-41 nanocomposites containing PdO species that are dispersed on an MCM-41 support using trans-$[PdCl_2(PEt_3)_2]$ as the source of metal [21]. Botas et al. prepared Fe_2O_3/SiO_2 catalysts by immobilization of iron species on SBA-15 [22]. The bimetallic mixed oxides–SBA-15 nanocomposites were prepared by Fulvio et al. using SBA-15 as a support and suitable metal containing reagents [23].

However, most of the surface of typical mesoporous silicas are covered by silica walls. This will influence the composite's catalytic activity. In order to overcome this disadvantage, mesoporous silica (MS) spheres are used to load pure metal oxide nanoparticles or their mixed oxides. MS spheres have slit-like mesopores, and most of the surface consists of mesopores. With mesopores serving as a confined reactor or growing space, the loaded nanocrystals showed a narrow size distribution and an obvious quantum confinement effect [24]. Moreover, the slit-like mesopores were very advantageous in terms of allowing access to reactants and for the release of reaction products.

In this paper, we demonstrate the confined growth of CuO, NiO, and Co_3O_4 nanocrystals in the pores of MS spheres with the help of polyelectrolyte (PE) multilayers. The metal oxide nanocrystals were synthesized by calcination method using urea hydrolysis. And cyclic voltammograms (CV) were used to investigate the catalytic performance of the composite microspheres.

2. Experimental

2.1. Materials

All the chemicals were of analytical grade and used without any further purification. N-hexadecylamine was purchased from Sigma–Aldrich Chemicals Co. Poly(allylamine hydrochloride) (PAH, M_W 70,000 Da) and poly(sodium-p-stryrenesulfonate) (PSS, M_W 70,000 Da) were purchased from Alfa Aesar Co., Ltd.

* Corresponding authors. Tel.: +86 21 64252022; fax: +86 21 64250624.
E-mail addresses: yhzhu@ecust.edu.cn (Y. Zhu), czli@ecust.edu.cn (C. Li).

0925-8388/$ – see front matter © 2010 Elsevier B.V. All rights reserved.
doi:10.1016/j.jallcom.2010.11.175

Tetraethoxysilane (TEOS) and all other chemicals were purchased from Shanghai Chemical Reagent Co. All solutions for adsorption and analysis were prepared with double distilled water.

2.2. Synthesis of mesoporous silica (MS) spheres

Mesoporous silica spheres were synthesized as described by the literature [25] with a little modification. Briefly, 1 g of hexadecylamine was dissolved in a mixed solution including 100 mL isopropanol and 90 mL double distilled water to form a clear solution. Then 1.4 mL ammonia was added, which was followed by the addition of 5.8 mL of tetraethoxysilane (TEOS). The mixture was homogenized and kept at room temperature overnight. The resulting white precipitate was collected by filtration of the reaction mixture, washed with ethanol three times and then with the distilled water twice, and dried at ambient temperature. The templates were removed by calcination at 600 °C for 6 h in flowing air. To expand the pore size of MS spheres, a mixed solution with three ingredients including NaCl, LiCl and KNO_3 was adopted. MS spheres were soaked in the above salts solution and dispersed with ultrasonic. The mixture was dried at 80 °C, and then calcined at 435 °C for 2 h in nitrogen atmosphere.

2.3. Immobilization of M^{2+} (Cu^{2+}, Ni^{2+}, and Co^{2+}) in MS spheres

0.2 g of MS powders were impregnated with 6 mL of $Cu(NO_3)_2$, $Ni(NO_3)_2$, and $Co(NO_3)_2$ with the metal molar concentration of 0.1 M, respectively. After shaking at room temperature for 24 h, the treated particles were separated by centrifugation, and washed with doubly distilled water for several times, in order to separate the M^{2+} (Cu^{2+}, Ni^{2+}, and Co^{2+}) unabsorbed from the particles.

2.4. Coating the M^{2+} (Cu^{2+}, Ni^{2+}, and Co^{2+})-adsorbed mesoporous silica spheres with polyelectrolytes (PE)

Polyelectrolytes were assembled by the sequential deposition of PAH and PSS onto M^{2+} (Cu^{2+}, Ni^{2+}, and Co^{2+})-adsorbed mesoporous silica spheres using the layer-by-layer (LbL) technique [26]. Briefly, the as-prepared M^{2+} (Cu^{2+}, Ni^{2+}, and Co^{2+})-adsorbed MS particles were dispersed in 6 mL of PAH (1 g L^{-1}) containing 0.5 M NaCl. After initially depositing a layer of PAH, PSS (2 g L^{-1}) in 0.5 M NaCl were subsequently adsorpted. Adsorptions of PAH and PSS were performed at room temperature for 20 min. After each adsorption step, excess PE was separated by centrifugation, and washed with doubly distilled water for several times.

2.5. Synthesis of CuO, NiO, and Co_3O_4 nanocrystals in mesoporous silica (MS) spheres

The encapsulated particles were finally dispersed in urea solution at a concentration of 0.1 M. The mixtures were then heated to 95 °C and dried at the same temperature for 24 h to obtain the solid sample (assigned as as-prepared-1, as-prepared-2, and as-prepared-3, respectively). Then the as-prepared samples were further calcined at 550 °C in air for 2 h. The resulting samples were denoted as CuO/MS, NiO/MS, and Co_3O_4/MS, respectively.

2.6. Characterization

Scanning electron microscope (SEM) image was obtained using a JEOL JSM-6360LV instrument. The samples surfaces were coated with gold before the SEM measurements. Wide-angle (10–80°, 40 kV/200 mA) X-ray powder diffraction (XRD) data were recorded on a Rigaku D/max 2550 VB/PC diffractometer using nickel-filtered CuKα radiation with wavelength λ = 1.5406 Å. Adsorption–desorption measurements were conducted on a Micromeritics ASAP 2010 apparatus at 77 K using nitrogen as the adsorption gas. The surface areas were calculated by the Brunauer–Emmett–Teller (BET) method. And the pore diameters were calculated by the Barrett–Joyner–Halenda (BJH) method. High resolution transmission electron microscope (HRTEM) was performed on a JEOL JEM 2100F instrument using an acceleration voltage of 200 kV to characterize composite microspheres. The TEM specimens were prepared by dripping and drying the ethanol suspension of the samples on carbon-coated microgrids. Energy dispersive X-ray spectrum (EDS) (Falcon, EDAX) was recorded to determine the composition of the composite microspheres. Thermogravimetric analysis (TGA) of the samples was performed in air on a Mettler Toledo TGA-SDTA 851e from 95 to 550 °C with a heating rate of 10 °C/min. The cyclic voltammograms (CV) were performed by using a CHI 660C workstation (CH Instruments, Chenhua, Shanghai, China) connected to a personal computer. A three-electrode configuration was employed, consisting of a modified glassy carbon electrode (GCE) (3 mm in diameter) serving as the working electrode, and Ag/AgCl electrode (3 M KCl) and platinum wire serving as the reference and counter electrodes, respectively.

2.7. Electrochemical tests

The working electrode was prepared as follows: prior to modification, GCE was carefully polished with 1.0 μm, 0.3 μm and 0.05 μm α-alumina powders in sequence, rinsed thoroughly with double distilled water between each polishing step, sonicated in ethanol and double distilled water for 5 min respectively and dried with nitrogen. 15 μL of 0.5% Nafion solution diluted in double distilled water was placed on the surface of the GCE, and it was allowed to dry at room temperature (drop coating). Then, about 20 mg of samples were dispersed in 2 mL double distilled water with a few minutes of ultrasonication to form well-dispersed mixture. The surface of the Nafion/GCE was casted by 10 μL of the mixture and dried at room temperature (25 °C). All electrochemical experiments were carried out at room temperature using 6 M KOH as electrolyte solution. The electrodes were cycled from 0 to −0.8 V (CuO/MS) or −0.6 V (NiO/MS or Co_3O_4/MS) at a scan rate of 50 mV/s.

3. Results and discussion

A typical procedure for the confined growth of CuO, NiO, and Co_3O_4 nanocrystals in the mesopores of the MS spheres is shown in Fig. 1. The MS spheres were impregnated with $Cu(NO_3)_2$, $Ni(NO_3)_2$, and $Co(NO_3)_2$ solution, resulting in immobilization of M^{2+} (Cu^{2+},

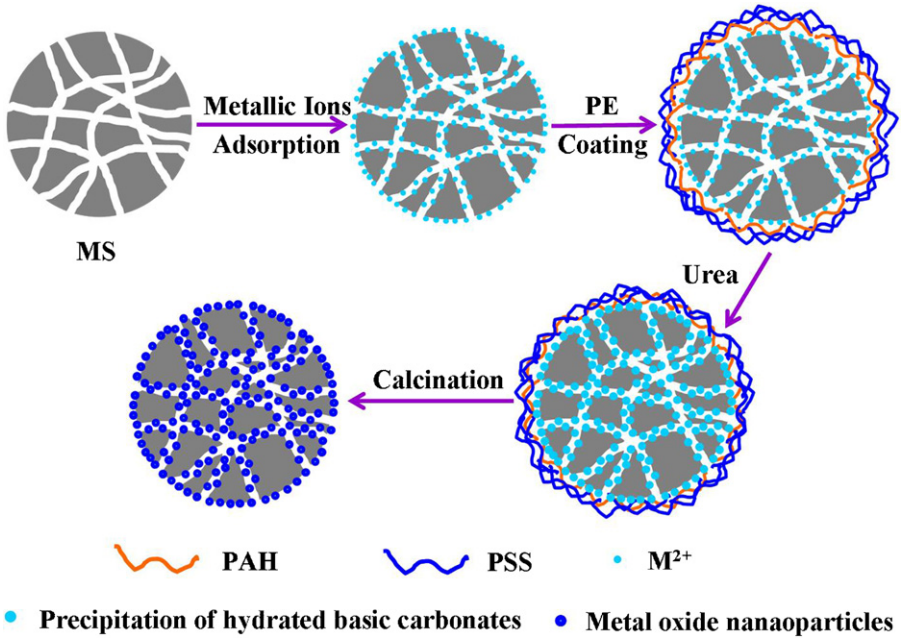

Fig. 1. Illustration of procedures for the confined growth of CuO, NiO, and Co_3O_4 nanocrystals in the mesopores of the MS spheres.

Ni^{2+}, and Co^{2+}) onto the Si–OH groups inside the MS spheres to form Si–O–M bonds due to the electrostatic interaction between M^{2+} and Si–OH. After coating with the PAH/PSS mutilayers, the M^{2+}-loaded MS spheres of core–shell structure were dispersed in urea solution to form the precipitation of hydrated basic carbonates. Finally, the metal oxides (CuO, NiO, and Co_3O_4) nanoparticles were prepared by calcination.

Fig. 2 shows SEM images and size distribution of MS spheres. Particles with a standard deviation below 10% are considered to be monodispersed [27]. The uniform spherical particles with an average size of 1.3 (±0.1) μm and good dispersion were clearly observed.

The XRD patterns of MS, CuO/MS, NiO/MS and Co_3O_4/MS are shown in Fig. 3. The broad feature at 22° in Fig. 3(a) is due to amorphous silica. All the other reflection peaks can be indexed as monoclinic CuO (Joint Committee on Powder Diffraction Standards (JCPDS) card, no. 89-5899) (Fig. 3(b)), cubic NiO (JCPDS card, no. 78-0643) (Fig. 3(c)), and cubic Co_3O_4 (JCPDS card, no. 78-1969) (Fig. 3(d)), respectively. The results indicate that the metal oxides (CuO, NiO or Co_3O_4) have been successfully loaded on MS spheres.

The nitrogen adsorption isotherms of samples are shown in Fig. 4 and the parameters derived from these isotherms are listed in Table 1. It can be seen that in all cases, the isotherms are of type IV according to the IUPAC classification and exhibit H3-type hysteresis loops, characteristic of samples with slit-like mesopores [26]. The results indicate that the structure of composite microspheres is still mesoporous. The pore size distributions (PSD) (Fig. 5) show that the average mesopore diameter decreases after loading the metal oxides, suggesting that the metal oxides (CuO, NiO or Co_3O_4) have been confined in the mesopores of MS spheres. The specific surface areas of composite microspheres are higher than that of MS spheres. It is due to the load of the metal oxide nanoparticles on MS spheres.

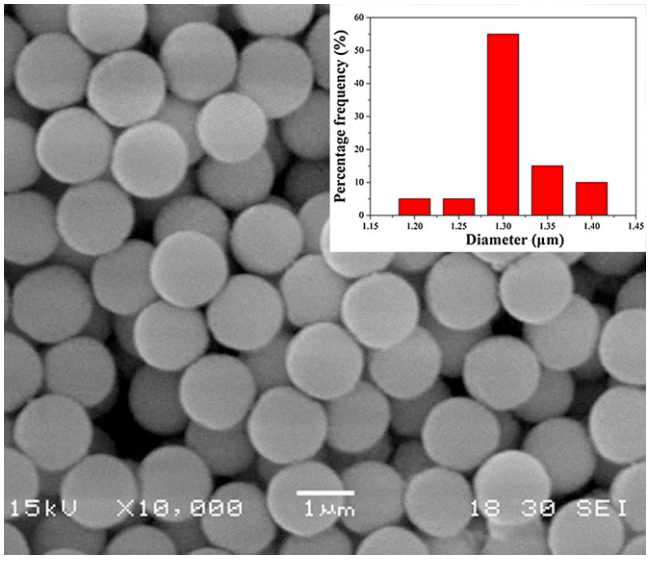

Fig. 2. Scanning electron microscope (SEM) image of as-prepared MS spheres (Inset: the corresponding size distribution).

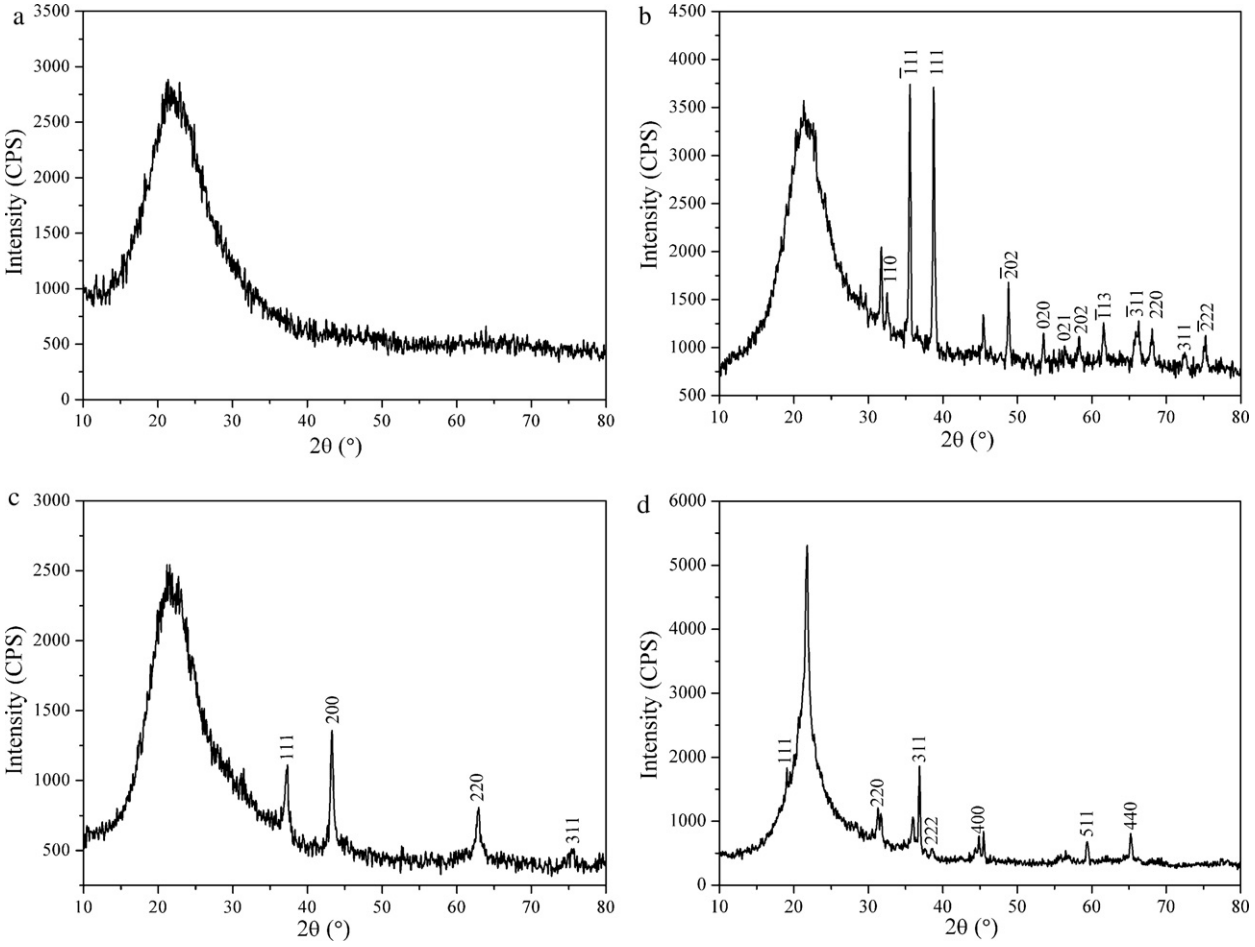

Fig. 3. XRD patterns of (a) MS, (b) CuO/MS, (c) NiO/MS and (d) Co_3O_4/MS.

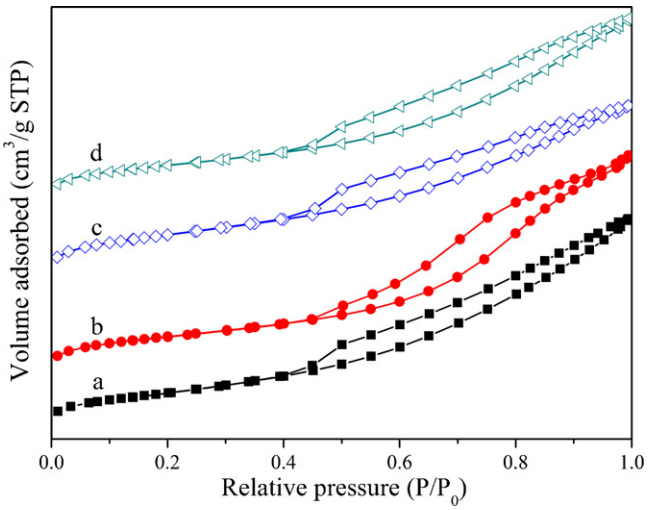

Fig. 4. Nitrogen adsorption–desorption isotherms of (a) MS, (b) CuO/MS, (c) NiO/MS, and (d) Co_3O_4/MS.

Table 1
Structural properties of (a) MS, (b) CuO/MS, (c) NiO/MS and (d) Co_3O_4/MS.

Sample	D_{BJH} (nm)	S_{BET} (m^2/g)
MS	22.49	46.24
CuO/MS	3.21, 6.09	173.2
NiO/MS	3.69	198.7
Co_3O_4/MS	3.59	167.4

Note: S_{BET}, specific surface area by BET; D_{BJH}, pore size by BJH.

Fig. 6 shows the representative TEM images of a composite microsphere (a) and the corresponding cross section ((b) and (c)). It could be observed that composite microsphere retained spherical morphology, indicating good dispersion. A few external metal oxide particles exist outside of the channels (Fig. 6(a)). It may explain that the use of elevated temperature results in the premature formation of large metal oxide particles outside of the mesopores. The metal oxide nanoparticles are confined in the pores of the MS spheres (Fig. 6(b) and (c)). This was consistent with the results in Fig. 5. The different diameters of composite microspheres and the knife marks in the same direction were caused by section. EDS was performed to determine the composition of the composite microspheres. The weight content of metal oxide nanoparticles (CuO, NiO, and Co_3O_4) in composite microspheres is 5.48%, 6.20%, and 15.77%, respectively.

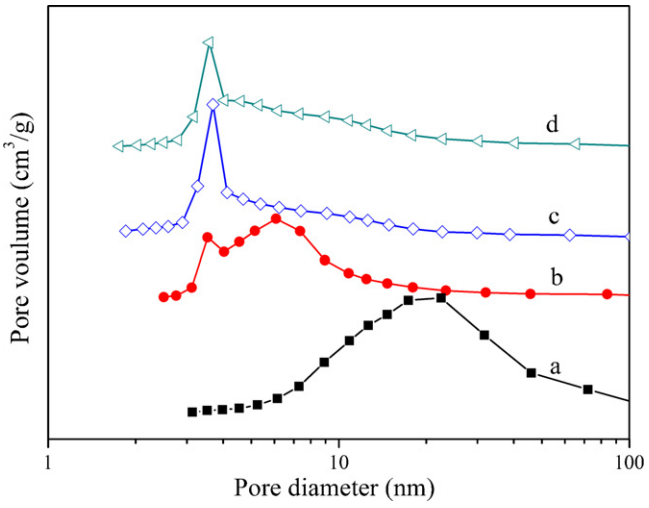

Fig. 5. The pore size distributions of (a) MS, (b) CuO/MS, (c) NiO/MS, and (d) Co_3O_4/MS.

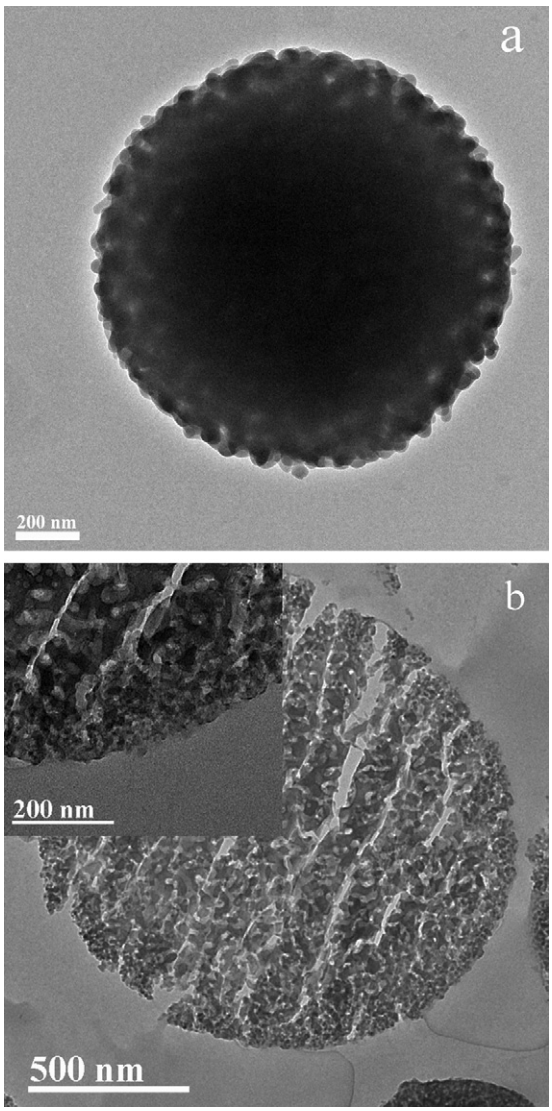

Fig. 6. Representative TEM images of (a) a composite microsphere and (b) the corresponding cross section (Inset: the amplified region of part (b)).

X-ray diffraction (XRD) and thermal gravimetric analysis (TGA) measurement was carried out to study the formation mechanism of the CuO phase.

Fig. 7 shows the XRD pattern of as-prepared-1. It indicates that the sample consisted of a mixed phase of $Cu_2(OH)_2CO_3$ and urea. The diffraction peaks can be indexed to both phases with the monoclinic $Cu_2(OH)_2CO_3$ (JCPDS card, no. 76-0660) and the tetragonal urea (JCPDS card, no. 72-1196). After calcination of as-prepared-1 at 550 °C for 2 h, the phase of well crystallized CuO with the monoclinic structure was obtained (Fig. 3(b)). The broad feature at 22° is also due to amorphous silica.

Fig. 8 displays the TGA curves of as-prepared-1. Three regions of weight loss were identified. The first one from 95 to 160 °C resulted in 6.3% weight loss, which is due to dehydration. The second one between 160 and 260 °C with a weight loss of 11.0% corresponds to the decomposition of $Cu_2(OH)_2CO_3$ and surplus urea [28–30]. The last one between 260 and 550 °C shows the weight loss of 2.7%, which is attributed to the decomposition of polyelectrolytes [31]. The remaining CuO/SiO_2 fraction was found to be 80.0 wt.%.

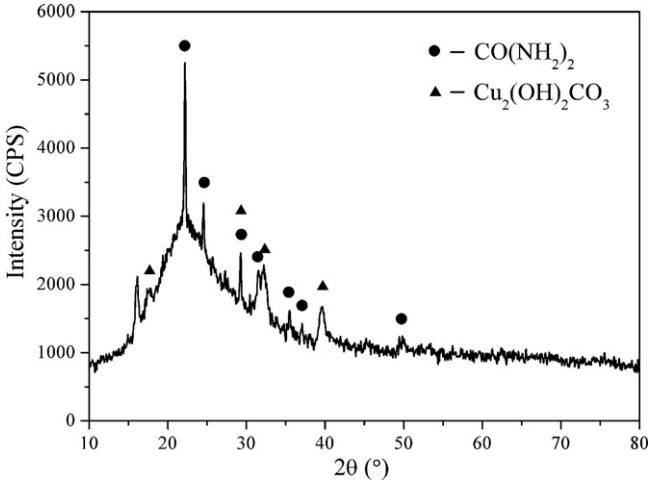

Fig. 7. XRD patterns of as-prepared-1.

The formation of CuO phase is believed to be similar to a mechanism proposed by Fernández et al. [32] and Shishido et al. [33,34]. The urea was hydrolyzed in heated water (>60 °C). The hydrolysis of urea proceeds in two steps, the formation of ammonium cyanate (Reaction (1)) as the rate determining step, and the rapid hydrolysis of cyanate to form ammonium carbonate (Reaction (2)). Hydroxide anions (OH^-) are also associated with the products of urea decomposition (Reaction (3)) and with the water dissociation reaction (Reaction (4)).

$$(NH_2)_2CO \rightarrow NH_4^+ + NCO^- \quad (1)$$

$$NCO^- + 2H_2O \rightarrow NH_4^+ + CO_3^{2-} \quad (2)$$

$$CO_3^{2-} + H_2O \rightarrow HCO_3^- + OH^- \quad (3)$$

$$H_2O \leftrightarrow H^+ + OH^- \quad (4)$$

Hydroxide anions (OH^-) and carbonate ions which could penetrate through the polyelectrolyte mutilayers are considered to be responsible for the precipitation of hydrated basic carbonates. The resulting precipitation is converted to stable CuO phase by calcination.

The formation mechanism of NiO phase is similar to that of CuO phase. But Co_3O_4 does not seem to follow the same path since some must convert from a 2+ charge in the precursor to a 3+ charge in the product while copper and nickel maintain the 2+ charge. The formation mechanism of Co_3O_4 appears to be more complex due to the change in oxidation state and is beyond the scope of the discussion in this paper.

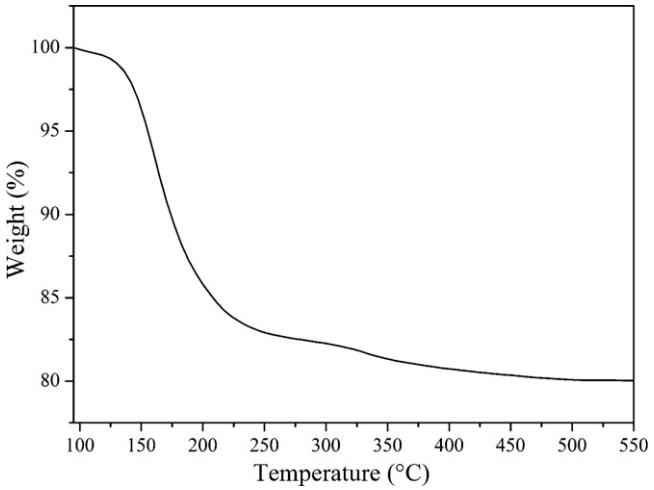

Fig. 8. TGA curves of as-prepared-1.

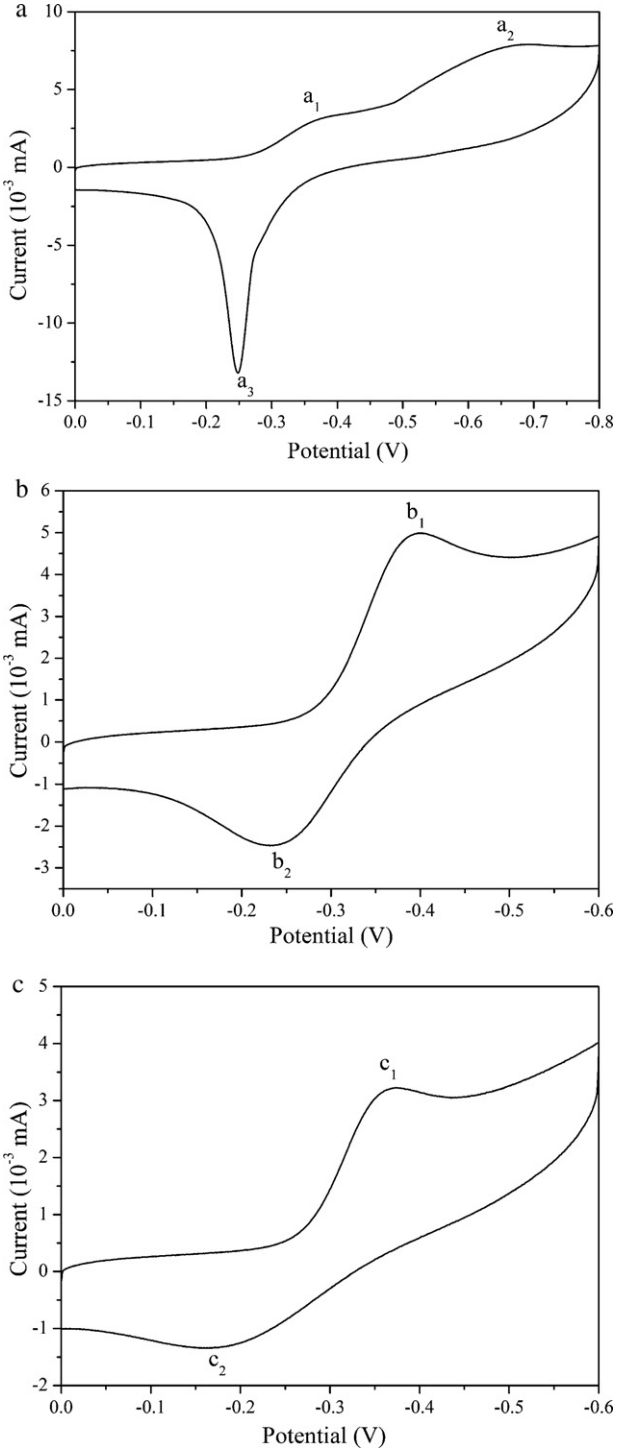

Fig. 9. Cyclic voltammograms of (a) CuO/MS/Nafion/GCE, (b) NiO/MS/Nafion/GCE and (c) Co_3O_4/MS/Nafion/GCE.

As we know, redox potentials of the catalysts are important parameters in determining the catalytic activity. And cyclic voltammetry is a strong tool to investigate the reversible redox ability of the catalysts [35]. Hence, the redox properties of CuO/MS, NiO/MS, and Co_3O_4/MS composite microspheres were explored with the aid of CV measurement, as shown in Fig. 9.

Fig. 9(a) shows the cyclic voltammogram of CuO/MS composite microspheres. As shown, two reduction peaks were observed at −0.36 V (peak a_1) and −0.65 V (peak a_2) during the negative potential scan. And during the positive potential scan, one oxidation peak was observed at −0.24 V (peak a_3). The catalytic behavior could be explained by the following mechanism [36]:

$$\text{Peak } a_1 : CuO + H_2O + e^- \rightarrow CuOH + OH^- \quad (5)$$

$$\text{Peak } a_2 : CuOH + e^- \rightarrow Cu + OH^- \quad (6)$$

$$\text{Peak } a_3 : Cu + 2OH^- \rightarrow Cu(OH)_2 + 2e^- \quad (7)$$

$$Cu(OH)_2 \leftrightarrow CuO + H_2O \quad (8)$$

Fig. 9(b) shows the cyclic voltammogram of NiO/MS composite microspheres. As shown, one reduction peak was observed at −0.39 V (peak b_1) during the negative potential scan. And during the positive potential scan, one oxidation peak was observed at −0.23 V (peak b_2). The catalytic behavior could be explained by the following mechanism [37,38]:

$$\text{Peak } b_1 : NiOOH + e^- \rightarrow NiO + OH^- \quad (9)$$

$$\text{Peak } b_2 : NiO + OH^- \rightarrow NiOOH + e^- \quad (10)$$

Fig. 9(c) shows the cyclic voltammogram of Co_3O_4/MS composite microspheres. As shown, one reduction peak was observed at −0.37 V (peak c_1) during the negative potential scan. And during the positive potential scan, one oxidation peak was observed at −0.17 V (peak c_2). The catalytic behavior could be explained by the following mechanism [39]:

$$\text{Peak } c_1 : Co_3O_4 + 4H_2O + 2e^- \rightarrow 3Co(OH)_2 + 2OH^- \quad (11)$$

$$\text{Peak } c_2 : 3Co(OH)_2 + 2OH^- \rightarrow Co_3O_4 + 4H_2O + 2e^- \quad (12)$$

The CuO/MS composites show the larger area of reduction or oxidation peak (Fig. 9(a)) than that in paper [40], suggesting the more electro redox active materials. And they often show more excellent catalytic activity probably because of the more catalytic active sites. So do the NiO/MS and Co_3O_4/MS composites.

The results show that CV is valuable for the investigation of catalytic performances of CuO/MS, NiO/MS, and Co_3O_4/MS composite microspheres. Therefore, CV of catalysts can be applied in selecting catalyst used for catalytic reaction.

4. Conclusions

In conclusion, a novel approach for the preparation of composite materials involving metal oxide nanaoparticles which have potential application in catalytic field is described. The metal oxides (CuO, NiO, or Co_3O_4) nanoparticles were confined in the mesopores of the MS spheres with the help of polyelectrolyte (PE) multilayers by calcination method using urea hydrolysis. The metal oxide (CuO, NiO, or Co_3O_4) nanoparticles were almost confined in the mesopores of the MS spheres and had good crystallinity. And the resulting composite microspheres with good dispersion are still mesoporous. Their catalytic performances were investigated with the aid of CV. Further investigation will lay emphasis on the application of these composite microspheres in catalytic field.

Acknowledgments

This work was supported by the National Natural Science Foundation of China (20925621, 20976054), the Key Project of Science and Technology for Ministry of Education (107045), the Innovation Program of Shanghai Municipal Education Commission (09ZZ58), the Program of Shanghai Subject Chief Scientist (08XD1401500) and the Program for Changjiang Scholars and Innovative Research Team in University (IRT0825).

References

[1] M. Epifani, T. Andreu, J. Arbiol, R. Díaz, P. Siciliano, J.R. Morante, Chem. Mater. 21 (2009) 5215–5221.
[2] C.S. Li, Y.N. Li, Y.L. Wu, B.S. Ong, R.O. Loutfy, J. Mater. Chem. 19 (2009) 1626–1634.
[3] Y.X. Rao, D.M. Antonelli, J. Mater. Chem. 19 (2009) 1937–1944.
[4] D. Pietrogiacomi, A. Magliano, P. Ciambelli, D. Sannino, M.C. Campa, V. Indovina, Appl. Catal. B: Environ. 89 (2009) 33–40.
[5] O.G.M. Flores, S. Ha, Appl. Catal. A: Gen. 352 (2009) 124–132.
[6] T.Y. Yang, K.N. Sun, Z.Y. Lei, N.Q. Zhang, Y. Lang, J. Alloys Compd. 502 (2010) 215–219.
[7] N. Du, H. Zhang, J.X. Yu, P. Wu, C.X. Zhai, Y.F. Xu, J.Z. Wang, D. Yang, Chem. Mater. 21 (2009) 5264–5271.
[8] A. Serra, E. Filippo, A. Buccolieri, M.D. Giulio, D. Manno, Sens. Actuators. B: Chem. 140 (2009) 563–567.
[9] N. Sokkalingam, G. Kamath, M. Coscione, J.J. Potoff, J. Phys. Chem. B 113 (2009) 10292–10297.
[10] A.F. Vatta, P.J. Waller, J.B. Githiori, G.F. Medley, Vet. Parasitol. 162 (2009) 306–313.
[11] W. Wang, Y. Xu, D.I.C. Wang, Z. Li, J. Am. Chem. Soc. 131 (2009) 12892–12893.
[12] L.Y. Chen, Z.X. Xu, H. Dai, S.T. Zhang, J. Alloys Compd. 497 (2010) 221–227.
[13] P.Y. Wu, X.J. Li, S.F. Ji, B. Lang, F. Habimana, C.Y. Li, Catal. Today 146 (2009) 82–86.
[14] H.R. Emamian, A. Honarbakhsh-raouf, A. Ataie, A. Yourdkhani, J. Alloys Compd. 480 (2009) 681–683.
[15] S. Ajaikumar, A. Pandurangan, Appl. Catal. A: Gen. 357 (2009) 184–192.
[16] E. Beyers, E. Biermans, S. Ribbens, K.D. Witte, M. Mertens, V. Meynen, S. Bals, G.V. Tendeloo, E.F. Vansant, P. Cool, Appl. Catal. B: Environ. 88 (2009) 515–524.
[17] M.Y. Cheng, C.J. Pan, B.J. Hwang, J. Mater. Chem. 19 (2009) 5193–5200.
[18] S. Sohrabnezhad, A. Pourahmad, J. Alloys Compd. 505 (2010) 324–327.
[19] L.L. Kong, B. Yan, Y. Li, J. Alloys Compd. 481 (2009) 549–554.
[20] C. Wang, Y.H. Ao, P.F. Wang, J. Qian, J. Hou, S.H. Zhang, J. Alloys Compd. 493 (2010) 410–414.
[21] J. Hernández-Pineda, J.M. del Río, E. Carreto, E. Terrés, J.A. Montoya, M. de Jesús Zuñiga-González, J. Morgado, J. Alloys Compd. 481 (2009) 526–530.
[22] J.A. Botas, J.A. Melero, F. Martínez, M.I. Pariente, Catal. Today 149 (2010) 334–340.
[23] P.F. Fulvio, S. Pikus, M. Jaroniec, ACS Appl. Mater. Interfaces 2 (2010) 134–142.
[24] H.F. Yang, Q.Y. Lu, F. Gao, Q.H. Shi, Y. Yan, F.Q. Zhang, S.H. Xie, B. Tu, D.Y. Zhao, Adv. Funct. Mater. 15 (2005) 1377–1384.
[25] Y.X. Li, Y.H. Zhu, C.Y. Li, X.L. Yang, C.Z. Li, Mater. Lett. 63 (2009) 1068–1070.
[26] Y. Kuroda, K. Kuroda, Sci. Technol, Adv. Mater. 9 (2008) 025018.
[27] T.M. Suzuki, M. Mizutani, T. Nakamura, Y. Akimoto, K. Yano, Micropor. Mesopor. Mater. 116 (2008) 284–291.
[28] M. Eichelbaum, R.J. Farrauto, M.J. Castaldi, Appl. Catal. B: Environ. 97 (2010) 90–97.
[29] J.W.H. Smith, P. Westreich, L.M. Croll, J.H. Reynolds, J.R. Dahn, J. Colloid Interface Sci. 337 (2009) 313–321.
[30] W.M. Shaheen, I.H.A.E. Maksod, J. Alloys Compd. 476 (2009) 366–372.
[31] A. Satti, P. Larpent, Y. Gun'ko, Carbon 48 (2010) 3376–3381.
[32] Y. Fernández, J.A. Menéndez, A. Arenillas, E. Fuente, J.H. Peng, Z.B. Zhang, W. Li, Z.Y. Zhang, Solid State Ionics 180 (2009) 1372–1378.
[33] T. Shishido, Y. Yamamoto, H. Morioka, K. Takehira, J. Mol. Catal. A: Chem. 268 (2007) 185–194.
[34] T. Shishido, M. Yamamoto, D.L. Li, Y. Tian, H. Morioka, M. Honda, T. Sano, K. Takehira, Appl. Catal. A: Gen. 303 (2006) 62–71.
[35] J.J. Zhu, Z. Zhao, D.H. Xiao, J. Li, X.G. Yang, Y. Wu, Electrochem. Commun. 7 (2005) 58–61.
[36] M. Kang, A.A. Gewirth, J. Phys. Chem. B 106 (2002) 12211–12220.
[37] C.Z. Yuan, B. Gao, L.H. Su, X.G. Zhang, Solid State Ionics 178 (2008) 1859–1866.
[38] H.F. Li, Y.F. Li, R.D. Wang, R. Cao, J. Alloys Compd. 481 (2009) 100–105.
[39] L. Tian, J.Y. Bian, B.B. Wang, Y.J. Qi, Electrochim. Acta 55 (2010) 3083–3088.
[40] A.G. Kong, H.W. Wang, X. Yang, Y.W. Hou, Y.K. Shan, Micropor. Mesopor. Mater. 118 (2009) 348–353.